Soft-x-ray emission and the local p-type partial density of electronic states in Y_2O_3: Experiment and theory

Donald R. Mueller*
National Institute of Standards and Technology, Gaithersburg, Maryland 20899

David L. Ederer and J. van Ek
Tulane University, New Orleans, Louisiana 70118

William L. O'Brien,† Qing Y. Dong,‡ Jianjun Jia,§ and Thomas A. Callcott
University of Tennessee, Knoxville, Tennessee 37996

(Received 20 June 1995; revised manuscript received 18 July 1996)

Photon-excited yttrium $M_{IV,V}$, and electron-excited oxygen K x-ray emission spectra for yttrium oxide are presented. It is shown that, as in the case of yttrium metal, the decay of M_{IV} vacancies does not contribute substantially to the oxide $M_{IV,V}$ emission. The valence emission is interpreted in a one-electron picture as a measure of the local p-type partial density of states. The yttrium and oxygen valence emission bands are very similar and strongly resemble published photoelectron spectra. Using local-density approximation electronic structure calculations, we show that the broadening of the Y-4p signal in yttrium oxide relative to Y metal are due to two inequivalent yttrium sites in Y_2O_3. Features present in the oxide, but not the metal spectrum, are the result of overlap (hybridization) between the Y-4p wave function and states in the oxygen 2s subband. [S0163-1829(96)07245-1]

INTRODUCTION

The electronic structure of yttria, Y_2O_3, has recently been examined by a first-principles self-consistent band-structure calculation[1] as well as via x-ray photoelectron spectroscopy.[2,3] The first-principles treatment[1] describes the electronic partial density of states in the valence and conduction region. We have extended these calculations to include contributions to the density of states from the shallow Y-4p and O-2s core levels. Soft x-ray emission spectroscopy provides a bulk-sensitive measure of the occupied electronic partial density of states which is complementary to the total density of state information provided by photoelectron spectroscopy. Yttrium M_V and oxygen K emission measurements, which are sensitive to the p-type partial density of states at the yttrium and oxygen sites, shall be presented. Previous measurements of the Y M_V emission spectrum of Y_2O_3 have been reported,[4] however, overlapping transitions into Y 3p vacancies contributed to the measured intensity in the valence region. The present measurement avoids this problem through selective excitation of the emission spectrum via a monochromatized photon beam.

In x-ray emission spectroscopy an electron or a photon beam is used to generate vacancies in the core levels of atoms within a specimen. The energy distribution of the x-rays emitted as electrons drop into core-level vacancies from occupied valence states depends upon the product of the matrix element connecting the initial core vacancy with the valence states and upon the local density of electronic states at the site of the initial core vacancy. The x-ray emission process obeys the dipole selection rule; consequently an x-ray emission spectrum also resolves the angular momentum of electronic states. Aside from a factor of photon energy cubed (which arises from the photon density of states and the dipole approximation) the matrix element connecting the initial and final states is often only weakly energy dependent over the limited energy extent of the valence band; particularly when the measurement is sensitive to valence levels of only one angular momentum symmetry.

Soft x-ray emission is insensitive to sample charging, because photons rather than low energy electrons are detected, which complicates photoelectron studies of insulating samples. In addition, photons have an absorption length in solids greater than the mean free path of low energy electrons which renders x-ray emission spectroscopy less surface sensitive than photoelectron spectroscopy. At the soft x-ray energies examined in this study atomic absorption data[5] may be used to estimate the average depth of sample probed:

$$z_{\mathrm{av}} = \cos(\theta_i)\cos(\theta_0)\,\frac{\int_0^\infty z\,\exp[(-\mu_i-\mu_0)z]\,dz}{\int_0^\infty \exp[(-\mu_i-\mu_0)z]\,dz}.$$

Here μ_i and μ_0 are the absorption coefficients of the ingoing and outgoing radiation while θ_i and θ_0 are the angles the incident and outgoing photon beams make with respect to the surface normal. The yttrium oxide M_V emission spectra presented below originate within the Y_2O_3 from an average depth of ~500 Å.

EXPERIMENT

The soft x-ray emission experiments were performed on beamline U-10A at the National Synchrotron Light Source at Brookhaven National Laboratory. The apparatus installed there incorporates facilities to generate core vacancies within a sample employing either an incident electron beam (0.5–5

keV), white light, or monochromatized synchrotron radiation. The monochromator is based on a variable-line-spaced grating design,[6] and is tunable in the range from 40 to 280 eV. For typical operating conditions yield a photon flux of $\sim 2\times 10^{13}$ photons/sec on a 2 mm^2 spot on the sample.

Light emitted from the sample was energy analyzed by a grating spectrometer and a computer-interfaced multichannel detector. The instrumentation has been described in more detail elsewhere.[7–9] The spectrometer resolution employed while measuring the spectra was 0.3 eV. The pressure in the sample chamber was below 10^{-11} Pa during the measurements.

The Y_2O_3 samples were pressed pellets of commercially available high-purity powder (99.99%). Emission from yttrium metal (99.9%) was also examined for comparison. The vacuum chamber was baked at a temperature of 450 K for 12 h prior to the measurements. This procedure is not expected to modify the sample stoichiometry as vacuum annealing at temperatures near 2000 K is required to decompose Y_2O_3 in vacuum.[2] The experiments were conducted with the samples at room temperature. There was no evidence of sample decomposition induced by the incident photon or electron beams. The samples were white when inserted into the vacuum chamber and remained white throughout the experiment. The energy calibration of the spectrometer was verified by examining the position of the Fermi edge in $L_{\mathrm{II,III}}$ emission spectra (Fermi edge to L_{III} transition energy: 72.8 eV) from a piece of aluminum foil mounted on the sample manipulator. Multiple order diffraction features were used to verify that the spectrometer calibration uncertainty was less than 0.2 eV over the entire energy range (50–200 eV) of the 600 line/mm grating. The $4p\rightarrow 3d$ transition in yttrium metal was observed at 132.2 $\pm$0.2 eV (93.8$\pm$0.2 Å) in agreement with the precise measurements by Crisp (93.55$\pm$0.03 Å).[10]

Several phenomena can alter or complicate the interpretation of x-ray emission spectra. Among these are the energy dependence of the spectrometer response, reabsorption of radiation emitted within the sample (self-absorption), and satellite emission features.

All data presented below have been corrected for the energy dependence of the spectrometer sensitivity which was determined by comparing the Bremsstrahlung profile in electron-beam excited spectra from Al and Cu samples with literature reports[11] of these profiles obtained with incident electrons of the same energy as those employed here. In any event the sensitivity of the spectrometer response does not vary significantly ($<$7%) over the relatively narrow energy range of the valence emission band. The valence emission is consequently insensitive to slight errors in our knowledge of the spectrometer response.

The emission spectra presented below have not been corrected for sample self-absorption. An energy-dependent estimate of the absorption coefficient within the compound can be made using atomic photoionization cross section data[5] and the sample density.[12] A correction factor to take into account the reabsorption of soft x rays within the sample can be expressed in terms of the absorption coefficients of the ingoing and emitted radiation and geometrical factors:

$$I_{\mathrm{corrected}}=I_{\mathrm{measured}}\{1+[\mu_0\sec(\theta_0)/\mu_i\sec(\theta_i)]\},$$

where θ_i is the angle between the sample's surface normal and the incident radiation beam and θ_0 is the angle between the normal and the detector. The quantities μ_i and μ_0 are, respectively, the absorption coefficients for the incoming and outgoing radiation beams. Over the energy range of the Y $3d_{5/2}\rightarrow$valence transitions this correction factor varies by approximately 3%. Due to uncertainty in the absorption data and the small magnitude of the effect no correction for self-absorption was applied.

Short-wavelength satellite contributions to emission spectra are known to arise from transitions in multiply excited atoms.[13] (Long wavelength satellites are generally rather weak.[14]) These multiply excited atoms may be formed through Auger decay of deeply bound core levels into a spectator vacancy and a vacancy in a level that is subsequently involved in radiative decay.[12,15] Use of a monochromatized photon beam to generate the core vacancies facilitates excitation at energies below those required to excite more tightly bound core levels, thereby eliminating the Auger mechanism of spectator vacancy generation. Excitation near threshold can also eliminate the possibility that direct multiple excitation or overlapping features from transitions involving more tightly bound states contribute to the emission spectra. The M_{V} threshold in Y metal is 155.8 eV. Photon energies near 170 eV were used to excite the yttrium spectra presented below. The bandwidth of the incident synchrotron radiation employed was 1.4 eV (full width at half maximum). Under these excitation conditions both overlapping emission features due to $3p\rightarrow 3d$ transitions and spectator-vacancy satellite contributions to the emission spectra are eliminated.

COMPUTATIONAL METHOD

For the calculation of the electronic structure of yttria the linear muffin tin orbital (LMTO) method within the atomic sphere approximation was used.[16] The sphere radii for the different species in the crystal were taken to be equal. Exchange and correlation effects for the electron gas were treated within the local density approximation of density functional theory, employing the exchange correlation potential as parametrized by Hedin and Lundquist.[17] Yttria crystallizes in the bixbyite structure[18] which is a body-centered-cubic structure (space group number 206, T_h^7). The Y atoms occupy positions $8a$ and $24d$, the oxygen atoms are at $48e$, and empty spheres were placed at $16c$ in order to improve the packing of the crystal. In total, the primitive cell contains 48 sites.

All electrons in the system were treated self-consistently. Since the Y-$4p$ states and the O-$2s$ states form narrow bands, these states were treated in a separate linearization panel. Thus the lower panel describes the Y-$4p$ and O-$2s$ derived bands, while the upper panel pertains to Y-$5s$, $5p$, $4d$, and O-$2p$ states. The basis for the Y atoms includes s, p, and d-type functions in each panel. Oxygen atoms and empty spheres are described with s and p-type functions in each panel. Since the spin-orbit effect greatly affects the Y $4p$ states, the spin orbit interaction was included in the Hamiltonian variationally.[19] Solutions for the low lying core states were obtained from the Dirac equation. The irreducible 1/48th part of the Brillouin zone was sampled with a tetra-

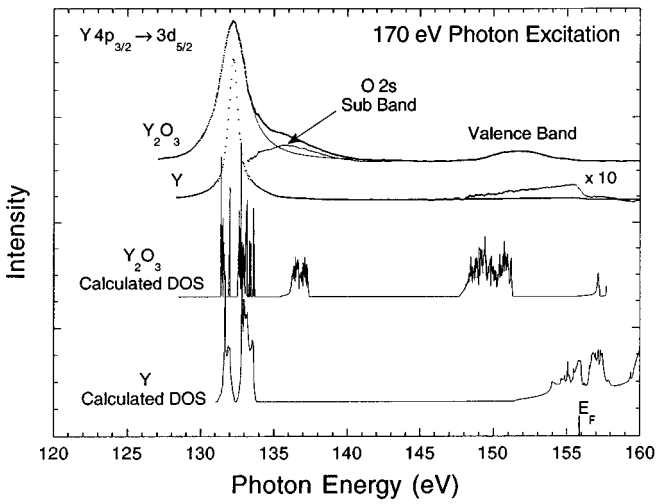

FIG. 1. Soft x-ray emission spectra for transitions into yttrium $3d$ vacancies in yttrium metal and in yttrium oxide shown as dotted curves in the upper half of the figure. For clarity the yttrium oxide data has been offset along the vertical axis as indicated. The yttrium metal data has been multiplied by a factor of ten in the valence region. The calculated total density of states for yttria and yttrium metal are shown as solid lines in the lower half of the figure. The doublet structure at photon energies of 131.5 and 134 eV is the DOS associated with the Y-$4p_{1/2}$ and $4p_{3/2}$ levels, respectively. States at energies greater than the Fermi energy, E_F, are unoccupied.

hedron method based on 220 k points. The total energy was converged to better than 0.1 meV in the self-consistent procedure. A similar calculation was performed for hexagonal-close-packed Y metal, at the experimental lattice constant and c/a ratio.

Yttria was found to be an insulator with a band gap of about 4.5 eV. The valence band is strongly dominated by the contribution of the O-$2p$ states. About 15 eV below the top of the valence band an O $2s$ subband with a width of approximately 1 eV is found, and around 19 eV below the top of the valence band the Y-$4p$ states produce a strongly peaked manifold, as shown in Fig. 1. The spin-orbit splitting between the $4p_{1/2}$ and $4p_{3/2}$ levels is about 1.2 eV, and the broadening of the manifold due to the inequivalent Y atoms is estimated to be 0.5 eV.

Yttrium metal is characterized by a 4.3 eV wide, $5s/4d$ dominated valence band, although right at the Fermi level the p-type density of states is significant. Around 23 eV below the Fermi level the $4p_{1/2}$ and $4p_{3/2}$-derived bands are split by about 1.2 eV.

The results found in Ref. 1 compare well with the calculated density of states (DOS) presented here, albeit that the band gap in Ref. 1 is only 2 eV wide. The width of the valence band (3.6 eV) and the atom resolved DOS in Ref. 1 agree very well with the present data.

RESULTS AND DISCUSSION

Figure 1 illustrates the measured emission spectra (the dotted curves in the upper half of the figure) and the calculated total density of states (the two curves in the lower half of the figure) from the valence region into a Y $3d_{5/2}$ core vacancy in yttria and in yttrium metal. The sharp edge in the yttrium metal soft-x-ray emission spectrum for an emitted photon energy of 155.9 ± 0.2 eV corresponds to the Fermi level and is in good agreement with our calculation. The peak at 132.3 ± 0.2 eV is due to photons emitted as electrons from the yttrium $4p_{3/2}$ level drop into an initial $3d_{5/2}$ vacancy. Photoemission measurements place the binding energy of the yttrium $3d_{5/2}$ level with respect to the Fermi level of the metal at 155.8 eV.[20] Transitions from the $4p_{1/2}$ to the $3d_{3/2}$ core states are allowed, but not observed in the experiment. Our calculation does include both the $4p_{1/2}$ and the $4p_{3/2}$-derived DOS, as can be seen in Fig. 1. The difference between the photoelectron binding energies of the $4p_{3/2}$ and $3d_{5/2}$ yttrium core states is 132.7 eV, which is consistent with the feature energies measured by x-ray emission. The measurements may also be subject to different relaxation shifts due to the response of other electrons in the sample to the creation and annihilation of vacancies.

In the soft-x-ray spectrum we might also expect to observe a second Fermi edge and a second core-core feature arising from transitions into $3d_{3/2}$ vacancies. However, neither a second Fermi edge at the binding energy of the $3d_{3/2}$ level (157.7 eV),[20] nor a second core-core transition ($3d_{3/2} \rightarrow 4p_{1/2}$) is observed. This observation is consistent with previous reports that the $3d_{3/2} \rightarrow 4p_{1/2}$ transition appears with approximately 2% the intensity of the corresponding $3d_{5/2} \rightarrow 4p_{3/2}$ transition for all the early $4d$ transition metals.[10]

The valence band in yttrium metal is derived largely from yttrium $5s$ and $4d$ states. The M_{V} spectra presented here are sensitive to states of p-type symmetry. The observed valence emission likely arises as a consequence of hybridization between the dominant valence states with the yttrium $5p$ levels, as observed in the calculated DOS for Y metal.

In the lower half of Fig. 1 the calculated total densities of states for the $4p$ shallow core states and the valence bands of the metal and the oxide is compared to the soft-x-ray emission from yttria and yttrium metal. The yttrium oxide x-ray spectrum exhibits a valence emission band centered near a transition energy of 152 eV. Furthermore, the $3d_{5/2} \rightarrow 4p_{3/2}$ core-core transition is broadened in the oxide with respect to its profile for yttrium metal because the yttrium in the oxide is distributed over two non-equivalent sites which results in slightly different $4p$ binding energies (about 0.5 eV). The DOS associated with the oxygen $2s$ subband in the oxide is also shown in the density of states and its presence in the x-ray emission spectrum is due to the interaction of Y-$4p$ electrons with oxygen atoms. This idea is reinforced by the experimental observations presented in the following paragraphs.

The chemical shift in core-level binding energy that accompanies compound formation is nearly the same for all core levels and it is observed that the core-core transition for the oxide is not shifted in energy with respect to the transition in the metallic sample. Note also that no additional emission peak due to the $3d_{3/2} \rightarrow 4p_{1/2}$ transition appears near the expected transition energy of 133.3 eV. This suggests that transitions into $3d_{3/2}$ vacancies do not contribute to the oxide emission spectrum either.

To verify this hypothesis, measurements were conducted for several values of the excitation photon energy, including

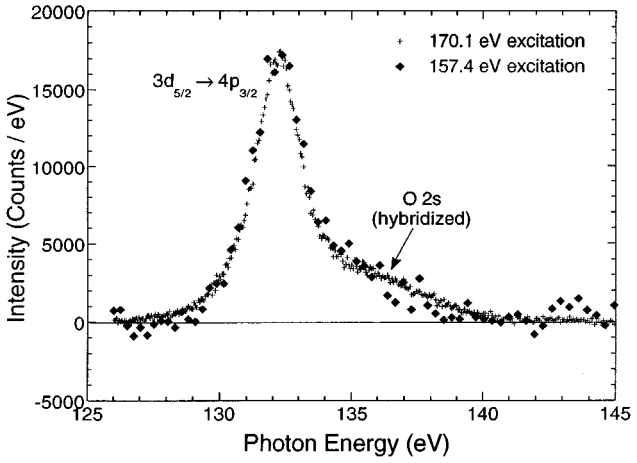

FIG. 2. The excitation-energy dependence of the yttrium oxide soft-x-ray emission spectrum in the region of the $3d \rightarrow 4p$ core-core transition.

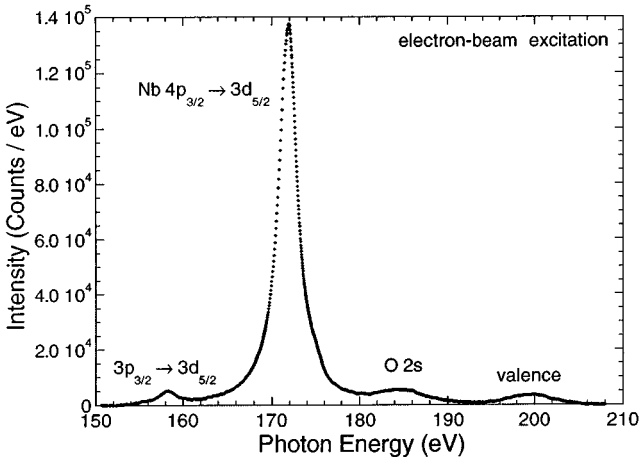

FIG. 3. Niobium M_V emission in Nb_2O_5. Note the weak emission feature near 185 eV.

170.1, 159.6, and 157.4 eV. Based on photoelectron spectroscopy the binding energy of the Y $3d_{5/2}$ level in Y_2O_3 is 158.6 eV, while the Y $3d_{3/2}$ level is characterized by a binding energy of 160.6 eV.[18–21] The incident beam energy was tuned to photon energies near the core-level threshold. For each excitation energy the core-core emission spectrum was observed. For an excitation energy of 159.6 eV the $3d_{3/2}$ threshold lies above while the $3d_{5/2}$ threshold lies below the center of the excitation-source energy distribution (FWHM $=1.4$ eV) and the excitation probability for the $3d_{3/2}$ level is greatly reduced (by approximately a factor of 9) relative to that of the $3d_{5/2}$ level. As illustrated in Fig. 2, no excitation-energy-dependent change in the profile of the emission spectrum was observed. This lack of change demonstrates that transitions into $3d_{3/2}$ vacancies do not contribute substantially to the oxide emission spectrum. (Note that the distinction between photoelectron binding energy and absorption threshold is unimportant for the case of yttrium oxide since the absorption edge chemical shift and the XPS chemical shift between the metal and the oxide are nearly the same.[2])

The emission spectrum induced by 157.4 eV incident radiation was also unaltered in appearance, although the total emission intensity was of course significantly reduced. For clarity the spectra presented in the figure were scaled so that the peak would appear with the same intensity.

The spectrum for yttria exhibits a feature near the $3d \rightarrow 4p$ core-core transition that does not appear in the metallic emission spectrum. The feature is centered approximately 15 eV below the valence band. Photoemission from yttrium oxide (Ref. 3, Fig. 6) also shows the oxygen-$2s$ derived band $\sim$15 eV below the valence band. In our calculations the Y-$4p$ and O-$2s$ levels were treated as band states. A look at the DOS (Fig. 1) clearly shows that the feature 15 eV below the valence band is due to the presence of the oxygen $2s$ band. From the angular momentum decomposed DOS it is seen that Y-$4p$ states contribute to the DOS at -16.5 eV, indicating significant overlap of Y-$4p$ states at the O site. In view of the bixbyite structure, this can be understood from the fourfold coordination of Y by oxygen atoms (distance $\sim$2 A). Inspection of the Y-$4p$ partial wave function as calculated with the LMTO method revealed that there is considerable overlap of the $4p$ states with the nearest neighbor oxygen sites.

For comparison Fig. 3 shows the emission spectrum of Nb_2O_5. The spectrum was obtained employing an incident 3 keV electron beam at a current density of $\sim$5 μA/mm^2. The niobium oxide spectrum also shows an emission peak approximately 15 eV below the upper valence emission band. Again the position of this feature is coincident with the relative location of the oxygen $2s$ peak and the valence band in photoemission data for Nb_2O_5 grown on an Nb surface.[22] The binding energy of the $4p$ level is greater for Nb than Y. This is reflected by the greater separation between the niobium $3d_{5/2} \rightarrow 4p_{3/2}$ core-core transition and the hybridized oxygen $2s$ band. Comparison of electron and photon excited spectra indicate that for the case of yttrium M_V emission short-wavelength satellite contributions to the spectrum appear only through slight broadening of the emission features and added intensity in the transition energy range between the valence emission band and the $3d \rightarrow 4p$ core-core transition. It is likely that satellite emission features do not contribute substantially to niobium M_V spectra either, particularly in light of the Lorentzian shape of the $3d \rightarrow 4p$ transition.

The data presented in Fig. 1 and Fig. 2 demonstrate that only transitions into Y $3d_{5/2}$ (M_V) vacancies contribute significantly to the yttrium emission spectra presented here. This is convenient for determination of valence partial density of state information in that it implies that deconvolution of the valence emission data into M_{IV} and M_V contributions is not required. In Fig. 4 we present the Y M_V and oxygen K valence emission data. The Y M_V emission was excited by an incident beam of 170 eV photons. The oxygen x-ray emission spectrum was measured in the fifth order of diffraction from the spectrometer grating and was excited by a 20 μA, 3 keV electron beam. The measured spectra have been divided by the cube of the photon energy to correct for the dependence of transition rate on the photon density of states in the final state within the dipole approximation. If the transition rate between the initial and final electronic states is otherwise not dependent on energy, the spectra are proportional to the yttrium p-type and oxygen p-type partial density of states. The oxygen K emission has been scaled to have the same

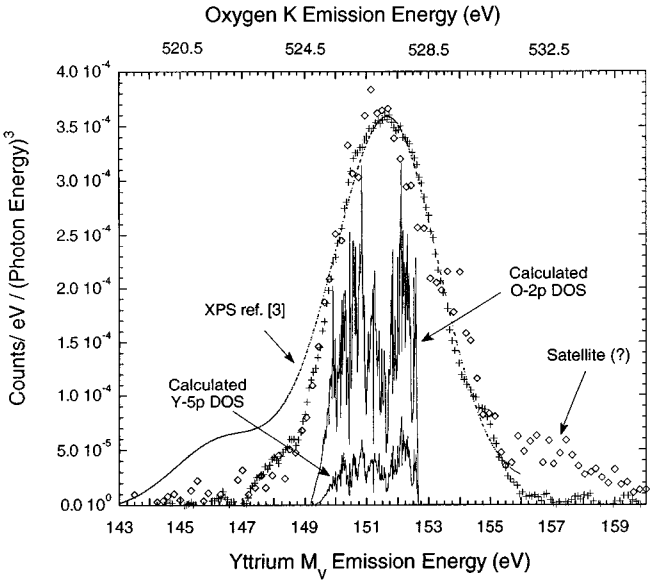

FIG. 4. The yttrium M_V valence emission band (crosses) compared with the oxygen K emission band (diamonds). The spectra have been divided by the cube of the photon energy to obtain the p-type local partial density of states. Also reproduced are photoelectron data and the calculated oxygen-2p partial density of states, as well as the yttrium-5p density of states.

intensity as the yttrium data. It has been displayed in the same graph as the yttrium emission to facilitate comparison of the two profiles. Also displayed is our calculated O-2p- and Y-5p-derived DOS. The photoelectron spectroscopy data from Ref. 3 is shown as the solid line, and has been scaled in intensity and displaced in energy to align the peak of the photoelectron spectrum with that of the x-ray emission. The calculated curves have also been aligned so that they are centered at the emission peak. The calculated Y-5p partial density of states is similar to the O-2p DOS, except that the Y-5p DOS is much less intense. Therefore, the valence band has a small contribution from Y-5p states, besides Y-5s, Y-4d, and O-2p. The similarity of the experimental spectra at the oxygen and yttrium sites indicates that the band structure is indeed pervasive, i.e., Y-5p states participate in the formation of the valence band of Y_2O_3.

Note that the high energy side of the oxygen emission spectrum probably includes satellite emission contributions, since it was excited with an electron beam substantially more energetic than the oxygen K threshold.

If the relaxation shifts due to screening of the electronic vacancies involved in x-ray emission and photoemission were the same, it would be possible to reference the x-ray emission data to the Fermi level via the binding energy of the Y $3d_{5/2}$ and O 1s levels. For metals, good agreement between the energy of features measured via photoemission and x-ray emission is usually obtained. This was the case for the yttrium metal data presented in Fig. 1. For insulators relaxation energies may displace x-ray emission and photoelectron spectra with respect to each other by several eV. In the absence of a Fermi edge that may be directly observed in the x-ray emission spectra we are thus unable to refer the spectra to an absolute binding energy scale. On the basis of the similarity in the shape of the oxygen and yttrium emission spectra we have aligned them to peak at the same location in Fig. 4.

The x-ray emission spectra are rather similar to the low binding energy (high transition energy) portion of the valence photoemission spectrum. At higher binding energies the valence photoemission exhibits a ''tail'' that is not reproduced in the x-ray emission. This difference may reflect a contribution to the photoelectron spectrum from states of other than p-type local symmetry; it may arise from a satellite in the photoelectron spectrum; or, as has been suggested,[1] it may reflect defect related electronic structure, particularly if the defects are localized at the surface (where the defect contribution would be unobserved in x-ray emission due to the difference in probe depth). There is also good agreement between the M_V x-ray emission spectra reported here and energy difference of the valence band emission peak and the yttrium 4p emission feature in photoelectron spectra (Ref. 2, Fig. 6).

The measured spectra are of course broadened with respect to the calculations presented in Ref. 1 both as a consequence of vacancy lifetime and instrumental response. The Lorentzian profile of the $3d_{5/2} \rightarrow 4p_{3/2}$ core-core transition and the sharp Fermi edge observed for the yttrium metal spectra imply that the broadening is mainly intrinsic. Considering experimental broadening the calculated Y-5p [Ref. 1, Fig. 2(c)] partial density of states is similar in overall width to the measured emission spectrum; however, the sharp change in the slope of the Y M_V spectrum at 149 eV implies that the experimental broadening is smaller than that required to smooth structure in the calculated Y-5p partial density of states to the level required for it to be unobserved in the experimental profile. The experiment implies a larger contribution to the density of states near the center of the valence band.

In a comparison between spectrographic results and ground state electronic structural calculations it must be understood that both photoemission and x-ray emission spectra measure transitions into or between excited states. The response of other electrons in the system to the creation and annihilation of vacancies could in principle change the measured distribution of emitted photons by other than a uniform relaxation shift. This however seems unlikely in light of the level of agreement between the oxygen and yttrium x-ray emission spectra as well as the photoelectron results. The agreement between the spectra requires that any such redistribution of the electronic states be the same at the yttrium and oxygen sites and in the description of the photoemission process.

SUMMARY

The x rays emitted during electronic transitions from the valence band into Y M_V and oxygen K level vacancies have been energy analyzed. The x-ray energy distributions so obtained were interpreted using yttrium p-type and oxygen p-type partial density of states information generated from a one-electron density functional calculation. The yttrium and oxygen valence spectra are very similar in shape and also conform closely to the x-ray photoelectron spectrum. Comparison of photoelectron data and our calculations with the yttrium x-ray emission spectrum in the region of the

$3d_{5/2}\rightarrow 4p_{3/2}$ transition reveals significant overlap of the Y-4p wave functions at the oxygen site, thereby hybridizing with the oxygen 2s subband. In view of the bixbyite structure for Y_2O_3 this points toward a strong interaction between Y atoms and the four oxygen atoms that are closest. As a result a signal is detected in the experimental spectrum at binding energies where the O-2s subband is located. Broadening of the $3d_{5/2}\rightarrow 4p_{3/2}$ transition with respect to Y metal is due to the two nonequivalent types of Y atoms in Y_2O_3. This inequivalence gives rise to a 0.5 eV difference in the position of the contributions to the $4p_{3/2}$-derived band. Niobium M_V emission data in Nb_2O_5 supports this interpretation.

ACKNOWLEDGMENTS

These measurements were supported at the University of Tennessee by National Science Foundation Grant No. DMR-8715430, by EPSCOR Grant No. DOE-EQSF (1993-95)-03 and by a Science Alliance Center of Excellence Grant from the University. The National Synchrotron Light Source is supported by DOE through Contract No. DE-AC02-CH00016. The authors are pleased to acknowledge assistance in handling the data from Robert Winarski, as well as helpful discussions with Dr. James MacLaren and Dr. Jose Jimenez-Mier.

*Deceased.
†Now at the Synchrotron Radiation Laboratory, Stoughton, WI 53589.
‡Now at Brookhaven National Laboratory, Upton, NY 11973.
§Now at the IMP, Inc., 2830 N. First St., San Jose, CA 95134.

[1] W. Y. Ching and Yong-Nian Xu, Phys. Rev. Lett. **65**, 895 (1990).
[2] F. Jollet, C. Noguera, M. Gautier, N. Thromat, and J-P. Duraud, J. Am. Ceram. Soc. **74**, 358 (1991).
[3] F. Jollet, C. Noguera, N. Thromat, M. Gautier, and J-P. Duraud, Phys. Rev. B **42**, 7587 (1990).
[4] L. M. Monastyrskiy, Phys. Met. Metall. **44**, 167 (1978).
[5] E. B. Saloman, J. H. Hubbell, and J. H. Scofield, At. Data Nucl. Data Tables **38**, 1 (1988).
[6] T. A. Callcott, W. O'Brien, J. Jia, Q. Y. Dong, D. L. Ederer, R. N. Watts, and D. R. Mueller, Nucl. Instrum. Methods, Phys. Res. A **319**, 128 (1992).
[7] T. A. Callcott, K. L. Tsang, C. H. Zhang, D. L. Ederer, and E. T. Arakawa, Rev. Sci. Instrum. **57**, 2680 (1986).
[8] T. A. Callcott, C. H. Zhang, K.-L. Tsang, E. T. Arakawa, D. L. Ederer, and J. Kerner, Nucl. Instrum. Methods B **40/41**, 398 (1989).
[9] T. A. Callcott, C. H. Zhang, D. L. Ederer, D. R. Mueller, J. E. Rubensson, and E. T. Arakawa, Nucl. Instrum. Methods Phys. Res. A **291**, 13 (1990).
[10] R. S. Crisp, J. Phys. F **12**, L163 (1982).
[11] T. J. Peterson, Jr. and D. H. Tomboulian, Phys. Rev. **125**, 235 (1962).
[12] *CRC Handbook of Chemistry and Physics*, 71th ed., edited by D. R. Lide (CRC Press, Boca Raton, FL, 1990), pp. 4–116.
[13] A. Meisel, G. Leonhardt, and R. Szargan, *X-Ray Spectra and Chemical Binding*, Springer Series in Chemical Physics Vol. 37 (Springer-Verlag, Berlin, 1989), p. 43.
[14] D. J. Nagel, Adv. X-Ray Anal. **13**, 183 (1970).
[15] N. Wassdahl, J.-E. Rubensson, G. Bray, P. Glans, P. Bleckert, R. Nyholm, S. Cramm, N. Martensson, and J. Nordgren, Phys. Rev. Lett. **64**, 2807 (1990).
[16] O. K. Andersen, Phys. Rev. B **12**, 3060 (1975)
[17] L. Hedin and B. I. Lundqvist, J. Phys. C **4**, 2064 (1971).
[18] R. W. G. Wyckoff, *Crystal Structures* (Interscience, New York, 1966).
[19] D. D. Koelling and B. N. Harmon, J. Phys. C **10**, 3107 (1977).
[20] G. P. Williams, *Center for X-Ray Optics X-Ray Data Booklet*, PUB-490, edited by Douglas Vaughn (Lawrence Berkeley Laboratory, University of California, Berkeley, 1986), pp. 2-5–2-4.
[21] C. E. Moore, *Atomic Energy Levels As Derived From the Analyses of Optical Spectra*, Natl. Bur. Stand. Ref. Data Ser., Natl. Bur. Stand. (U.S.) Circ. No. 35 (U.S. GPO, Washington, D.C., 1952), Vol. II.
[22] J. N. Miller, I. Lindau, P. M. Stefan, D. L. Weissman, M. L. Shek, and W. E. Spicer, J. Appl. Phys. **53**, 3267 (1982).